Available online at BCREC website: https://bcrec.id

Bulletin of Chemical Reaction Engineering & Catalysis, 18 (2) 2023, 200-209

Research Article

Synthesis, Structural Characterization，DFT，Hirschfeld Surface and Catalytic Activity of a New Zn(II) Complex of 4-Acetylbenzoic Acid

Li-Hua Wang[1]*, Hao-Wen Tai[2]

[1]College of Biology and Oceanography, Weifang University, Weifang 261061, P. R. China
[2]School of Science and Technology, Hong Kong Metropolitan University, Kowloon District, Hong Kong, P. R. China.

Received: 24th March 2023; Revised: 8th May 2023; Accepted: 8th May 2023
Available online: 10th May 2023; Published regularly: July 2023

Abstract

A new Zn(II) complex of 4-acetylbenzoic acid, namely $[ZnL_2(H_2O)_2]$ (1) (HL = 4-acetylbenzoic acid) has been synthesized in water-ethanol (v:v = 1:2) solution using zinc acetate dihydrate, 4-acetylbenzoic acid, and NaOH as reactants. The structure of complex (1) has been characterized by IR and X-ray single-crystal diffraction. X-ray diffraction analysis of complex (1) reveals that the Zn(II) ion is six-coordinated in a distorted octahedral coordination geometry with four carboxylic O atoms from two different bidentate 4-acetylbenzoic acid ligands (O1, O2, O1a, O2a) and two O atoms from two coordinated water molecules (O4 and O4a). Complex (1) forms 1D chained structure by the intermolecular and intramolecular O-H···O hydrogen bonds, and further forms a three-dimensional network structure by the π-π interaction of benzene rings and intermolecular O-H···O hydrogen bonds. The singlet ground-state geometry of the complex (1) were optimized using the PBE0 functional. The intermolecular interactions of complex (1) were quantitatively analysed by 3D Hirschfeld surface analysis and associated 2D fingerprint plots. The catalytic activity of complex (1) has been tested for the oxidation of benzyl alcohol under O2 atmosphere.

Keywords: 4-Acetylbenzoic acid; Zn(II) complex; Synthesis; Structural characterization; DFT computation; Hirschfeld surface; Catalytic activity

How to Cite: L.-H. Wang, H.-W. Tai, (2023). Synthesis, Structural Characterization，DFT，Hirschfeld Surface and Catalytic Activity of a New Zn(II) Complex of 4-Acetylbenzoic Acid. *Bulletin of Chemical Reaction Engineering & Catalysis*, 18(2), 200-209 (doi: 10.9767/bcrec.17747)

Permalink/DOI: https://doi.org/10.9767/bcrec.17747

1. Introduction

Zinc complexes have been one of the research topics of coordination chemists in recent years because to their excellent properties in fluorescence [1,2], anticancer activity [3,4], antiepileptic drug [5], antibacterial activity [6,7], antioxidative property [8], ON-OFF probe [9], gastroprotective activity [10], inorganic photosensitizer [11], DNA binding activity [12], nonlinear optical property [13], magnetic property [14], and electrochemical property [15,16]. It is worth mentioning that zinc complexes have also

* Corresponding Author.
Email: taixs@wfu.edu.cn (L.-H. Wang)
Telp: +86-536-8785286, Fax: +86-536-8785286

showed potential applications in their catalytic activity, such as: oxidation of benzyl alcohol [17,18], catalytic reduction of CO_2 [19], chemical fixation of CO_2 into cyclic carbonates [20], ring opening reaction of epoxide with amine [21], cyanosilylation of aldehydes [22], stereoselective ring opening polymerization of rac-lactide [23], A^3 coupling reaction [24], photodegradation of organic dye pollutants [25], etc.

We have synthesized some Zn(II) complexes and investigated their structure and properties [26-29]. Meanwhile, we also conducted a preliminary investigation of the catalytic activity of some metal complexes [30-35]. Up to now, there do not have report on the synthesis, crystal structure and catalytic property of 4-acetylbenzoic acid metal complexes. To continue the research in the novel structure and catalytic property of metal complexes, we synthesized and structural characterized a new Zn(II) complex using zinc acetate dihydrate, 4-acetylbenzoic acid (Figure 1), and NaOH as reactants.

2. Materials and Methods

2.1 Materials and Measurements

The materials of zinc acetate dihydrate (Jilin Chinese Academy of Sciences-Yanshen Technology Co., Ltd., 98%), 4-acetylbenzoic acid (Jilin Chinese Academy of Sciences-Yanshen Technology Co., Ltd., 98%), and NaOH (Jilin Chinese Academy of Sciences-Yanshen Technology Co., Ltd., 97%) were used as received. IR spectra were carried on a spectrophotometer (Tianjin Gangdong FTIR-850, KBr discs, range 4,000～400 cm^{-1}). The crystal data of complex (**1**) were obtained on a CCD area detector (Bruker CCD area detector, 296.15 K, multi-scan).

2.2 Synthesis of Complex (1)

A water (5 mL) solution of 0.1097 g zinc(II) acetate dihydrate (0.5 mmol) solid was added to a water-ethanol (15 mL, v:v = 1:2) solution of 0.0821 g 4-acetylbenzoic acid (0.5 mmol) solid and 0.020 g NaOH (0.5 mmol) solid. The mixture was heated to 70 °C and the temperature was held for 5 h with stirring before it was cooled to room temperature. The colourless crystals of complex (1) were formed after 20 days with yield 72%.

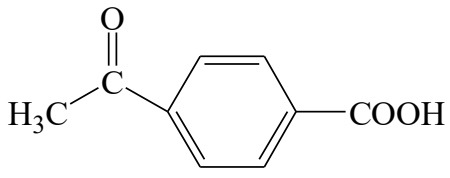

Figure 1. The molecular structure of 4-acetylbenzoic acid

2.3 Crystal Structure Determination

A suitable crystal (0.13 mm × 0.11 mm × 0.09 mm) of complex (1) was selected to collect data on a CCD area detector diffractometer. The crystal was kept at 296.15 K during data collection using Olex2 [36]. The structure was solved with the SHELXT [37] structure solution program using Intrinsic Phasing and refined with the SHELXL [38] refinement package using Least Squares minimisation. Crystallographic data of complex (1) are shown in Table 1. Crystallographic data for the structure reported in this paper has been deposited with the Cambridge Crystallographic Data Centre as supplementary publication No. CCDC 2222442. The CIF file can be obtained conveniently from the website: https://www.ccdc.cam.ac.uk/structures.

Table 1. Crystallographic data of complex (1)

Empirical formula	$C_{17}H_{15}O_7Zn$
Formula weight	396.66
Temperature/K	296.15
Crystal system	monoclinic
Space group	*C2/c*
a/Å	27.504(8)
b/Å	5.0047(13)
c/Å	12.086(3)
α/°	90
β/°	110.058(10)
γ/°	90
Volume/Å^3	1562.7(7)
Z	4
ρ_{calc}, mg/mm^3	1.686
μ/mm^{-1}	1.611
S	1.068
F(000)	812
Index ranges	$-32 \le h \le 32$, $-5 \le k \le 5$, $-14 \le l \le 13$
Reflections collected	17452
2θ/°	6.308-50.624
Independent reflections	1405 [*R*(int) = 0.1158]
Data/restraints/parameters	1405/1/127
Goodness-of-fit on F^2	1.068
Refinement method	Full-matrix least-squares on F^2
Final *R* indexes [I>=2*σ* (*I*)]	R_1 = 0.0593, wR_2 = 0.1446
Final *R* indexes [all data]	R_1 = 0.0809, wR_2 = 0.1609
Largest diff. peak/hole/e Å^{-3}	0.60/-0.93

2.4. Selective Oxidation of Benzyl Alcohol

The stainless-steel high-pressure reactor equipped with magnetic stirring and a temperature controller (10 mL) has been adopted to the selective oxidation of benzyl alcohol with oxygen. In a typical reaction, the complex (**1**) catalyst (20 mg) was suspended in the benzyl alcohol (1.0 mmol, 108.0 mg) and THF (7 mL). The reaction mixture was stirred at 2000 rpm with constant pressure (1-5 bar) of oxygen. After completion of the reaction, a sample of the reaction mixture was analyzed using gas chromatography (Varian star GC-6890) with SE-54 column and a fame ionization detector.

3. Results and discussion

3.1. Infrared Spectra

The infrared spectra of 4-acetylbenzoic acid and the complex (1) are given in Figure 2. The 4-acetylbenzoic acid ligand exhibits important bands at *ca.* 3265 (νO-H), 1728 (ν_{as}COO$^-$) and 1498 (ν_sCOO$^-$) cm^{-1}. In complex (1), the bands at *ca.* 3448 cm^{-1} indicates that the complex (1) contains water molecules, the ν_{as}COO$^-$ appears at 1618 and 1592 cm^{-1} and splits into two peaks, and the ν_sCOO$^-$ appears at 1398 cm^{-1}, indicating that the carboxylate of deprotonated 4-acetylbenzoic acid ligands adopt bidentate chelate coordination modes, which are consistent with the result of X-ray single-crystal diffraction analysis. The changes in the position of the major absorption peaks from the 4-acetylbenzoic acid ligand and complex (1) indicate that the 4-acetylbenzoic acid ligand is coordinated with the zinc ion.

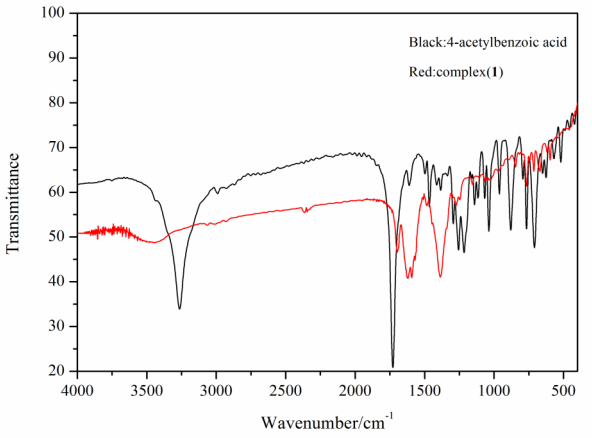

Figure 2. The infrared spectra of 4-acetylbenzoic acid and the complex (1)

3.2. Structural Description of Complex (1)

The coordination environment of Zn(II) in complex (1) is given in Figure 3. Selected bond lengths (Å) and angles (°) for complex (1) are listed in Table 2. Figure 4 and Figure 5 exhibits the 1D chained structure and the 3D network structure of complex (1) , respectively. The crystal structure of complex (1) contains one Zn(II) center, two 4-acetylbenzoate ligands and two coordinated water molecules (Figure 3). The carboxylate of deprotonated 4-acetylbenzoic acid ligands adopt bidentate chelate coordination modes. The Zn(II) center is six-coordinated in a distorted octahedral coordination geometry with four carboxylic O atoms (O1, O2, O1a, O2a, symmetry codes:a: 1-x, +y, 1/2-z) of two deprotonated 4-acetylbenzoic acid ligands and two O atoms (O4, O4a) of two coordinated water molecules. The basal plane is constructed by O1a, O2, O2a and O4, and the apical position is occupied by O1 and O4a. In complex (1), all oxygen atoms were disposed in *trans*, namely, O1 is *trans* to O1a, O2 is *trans* to O2a, and O4 is *trans* to O4a. The bond distances of Zn-O are 2.002(4) Å (Zn1-O1), 2.002(4) Å (Zn1-O1a), 1.982(3) Å (Zn1-O4), 1.982(3) Å (Zn1-O4a), 2.511(4) Å (Zn1-O2), and 2.511(4) Å (Zn1-O2a), respectively, which are consistent with those reported in the literature [39]. The dihedral angle of two benzene rings

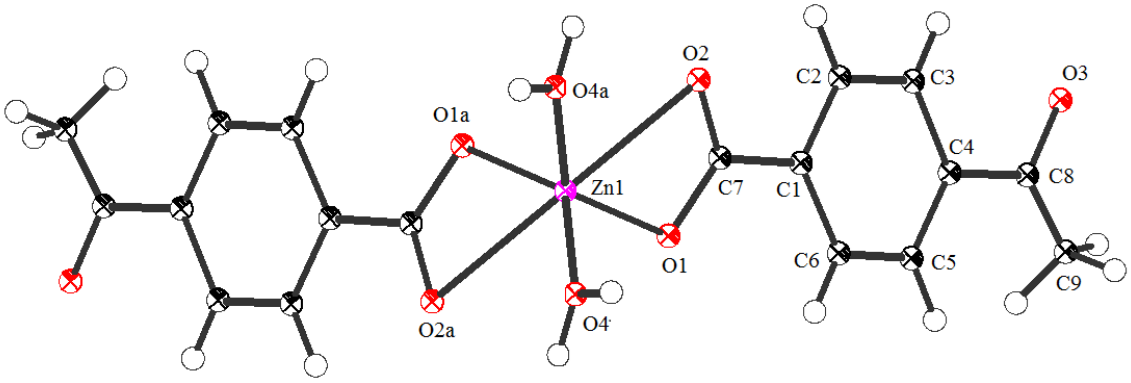

Figure 3. The coordination environment of Zn(II) in complex (1)

(C1-C2-C3-C4-C5-C6 and C1a-C2a-C3a-C4a-C5a-C6a) is 88.4°, showing that two 4-acetylbenzoate ligands are not coplanar. Complex (1) forms 1D chained structure (Figure 4) by the intermolecular and intramolecular O-H···O hydrogen bonds (O4-H4a···O1 and O4-H4b···O1), and further forms a three-dimensional network structure (Figure 5) by the π-π interaction of benzene rings and intermolecular O-H···O hydrogen bonds.

3.3. DFT Computation

The singlet ground-state geometry of complex (1) were optimized using the PBE0 functional [40]. The atomic basis set combines the 6-31G* basis set for C, H and O atoms with the Lanl2DZ effective core potential and valence basis set for Zn atoms. The vibrational analysis was performed at the same level and it confirms that the optimized geometry is stable. The vertical excitation energies were calculat-

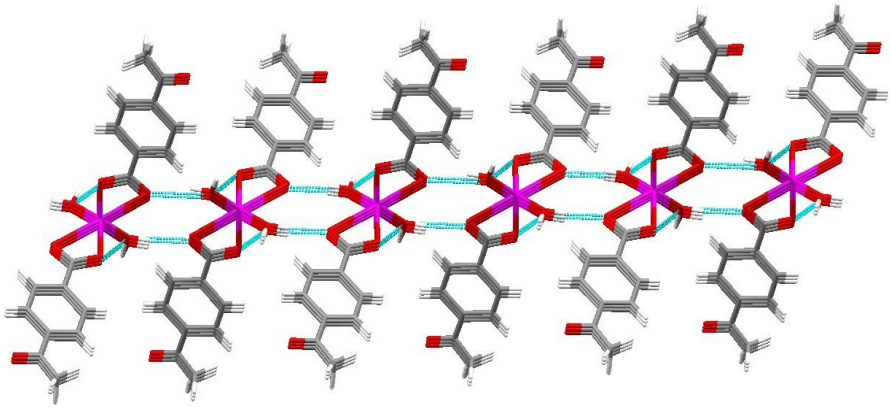

Figure 4. 1D chained structure of complex (1)

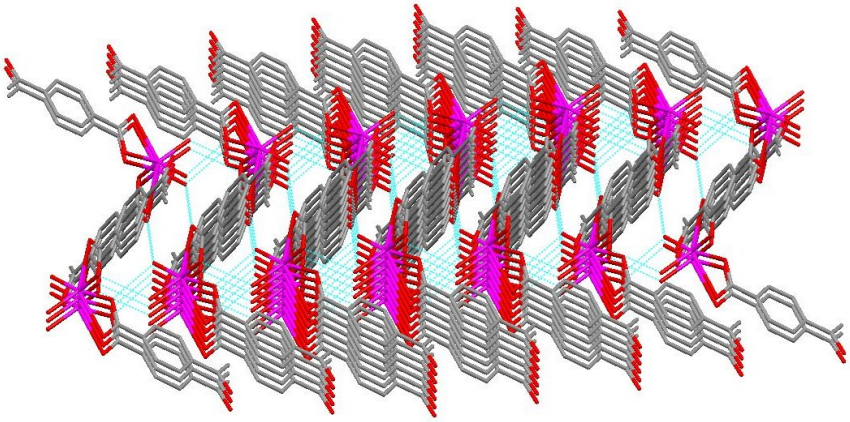

Figure 5. 3D network structure of complex (1)

Table 2. Selected bond lengths (Å) and bond angles (°) for complex (1)

Bond	*d*	Angle	(°)
Zn1-O1a	2.002(4)	O1-Zn1-O1a	99.3(2)
Zn1-O1	2.002(4)	O4a-Zn1-O1	136.22(14)
Zn1-O4a	1.982(3)	O1a-Zn1-O4	136.22(14)
Zn1-O4	1.982(3)	O4-Zn1-O1	100.86(15)
C7-O1	1.287(6)	O4a-Zn1-O1a	100.85(15)
C7-O2	1.248(6)	O4-Zn1-O4a	90.6(2)
		O2-C7-O1	119.8(4)

Symmetry transformations: a: 1-*x*, +*y*, 1/2-*z*.

ed at the TD-PBE0/6-31G(d)-Lanl2DZ theory of level based on the optimized geometry [41,42]. The solvation model employs the polarizable continuum model (PCM) with DMSO used as a solvent [43] because of the good solubility. All calculations were performed by the Gaussian 16 package [44]. The visual electron density of molecular orbital is realized by VMD package [45].

To get deep understanding of the ground state and excited state properties, DFT calculations were performed. The calculated geometric parameters of complex (1) are all in good agreement with the experimental results. There are two main absorption peaks for complex (1), i.e. 246.3 nm and 249.7 nm (Table 3) calculated based on the optimized geometry of ground state. The electron density distributions of the involved molecular orbitals are presented in Figure 6. The electron densities of all the involved molecular orbitals localize on the two 4-acetylbenzoate ligands. It indicates that these excitations show a mixed intraligand charge transfer (ILCT) / ligand-ligand charge-transfer (LLCT) character.

Table 3. Calculated absorption of the complex (1) in DMSO and the experimental data

Excited State	Excitation	λ_{cal} (nm)	*f*
7	HOMO-5→LUMO+1(32%)	249.7	1.066
	HOMO-4→LUMO(41%)		
	HOMO-2→LUMO(17%)		
8	HOMO-5→LUMO(43%)	246.3	0.223
	HOMO-4→LUMO+1(30%)		
	HOMO-3→LUMO (10%)		
	HOMO-2→LUMO+1 (13%)		

3.4. The Hirschfeld Surface of the Complex (1)

In order to better understand the distribution of electrons in the ligand. The Hirschfeld surface of the complex (1) was analyzed by the Crystal Explorer software 21.5. As shown in Figure 7, the original crystal structure unit, the Hirschfeld surfaces mapped over dnorm, di and de of the crystal (a-d), and the two-dimensional (2D) fingerprint plots represented overall and the top three interactions (H…H, O…H/H…O and C…H/H…C) are shown in (e-h). Based on the calculations, it can be concluded that the H…H contacts represented the largest contribution (39.7%) to the Hirschfeld surface, followed by O…H/H…O and C…H/H…C contacts with contributions of 32.5% and 12.2%, respectively. It's worth noting that the π-π stacking interactions play a subordinate role in forming the crystal for the C…C contacts with a Hirschfeld surface contribution percentage of 5.8%.

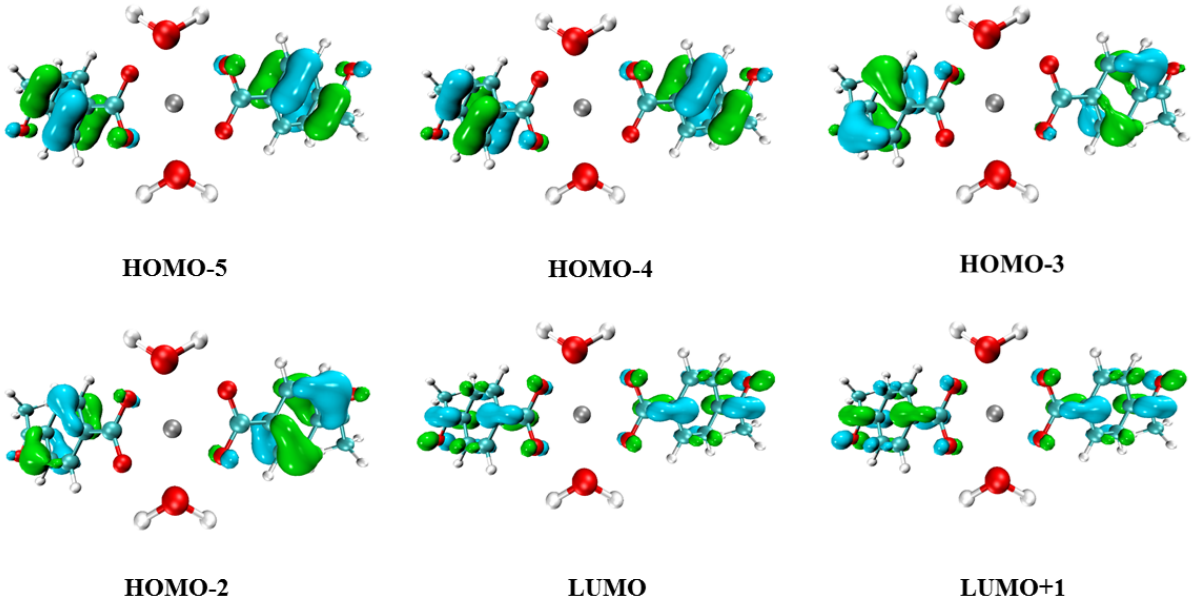

Figure 6. Electron density distributions of the involved molecular orbitals of the complex (1) (isovalue = 0.04 a.u)

3.5. Catalytic Activity Assessment of the Complex (1)

The results as shown in Table 4 depicts the conversion of benzyl alcohol and yield of benzaldehyde over complex (1) catalysts after a runtime of 1-3 h with O_2 as oxidant using THF as solvent. The benzyl alcohol conversion (9.3%) and benzyldehyde yield (3.2%) were low for the oxidation of benzyl alcohol at 100 °C within 2 h under 3 bar of O_2 without catalyst (Table 4, entry 1). The catalyst of complex (1) revealed remarkable increase in the conversion of benzyl alcohol with reaction temperature, time, and pressure (Table 4, entries 2–7). The benzyl alcohol conversions were 37.3% and 65.6% after a runtime of 2 h under 3 bar of O_2 at 90 °C and 100 °C, respectively (Table 4, entries 2 and 4). The conversions were 23.4%, 65.6%, and 85.6% at 100 °C under 3 bar after a runtime of 1, 2, and 3 h, respectively (Table 4, entries 3–5). The conversions of benzyl alcohol were 47.7%, 65.6%, and 69.5% under 1 bar, 3 bar and 5 bar at 100 °C within 2 h, respectively (Table 4, entries 4, 6, and 7). The highest benzaldehyde yield (66.3%) was obtained at 100 °C under 3 bar of O_2 after a runtime of 3 h. The yield of benzyldehyde over complex (1) was much higher than $[Zn_3(L_1)_4(L_2)_2(CH_3COO)_2]$ (50.8%, HL_1 = 6-phenylpyridine-2-carboxylic acid, L_2 = bis(4-pyridyl)amine), $[Ca(L)_2(H_2O)_2]_n$ (44.8%, L = 2-carboxybenzaldehyde), and $[BaL_2Cl_2]$ (42.7%, L = pyridine-2-carboxaldehyde-2-phenylacetic acid hydrazone) [17,46,47]. The calculated TOF of complex (1) based on the total Zn content was 5.9 h^{-1} at 100 °C under 3 bar of O_2 after a runtime of 3 h. TOF values of $[Zn_3(L_1)_4(L_2)_2(CH_3COO)_2]$, $[Ca(L)_2(H_2O)_2]_n$, and $[BaL_2Cl_2]$ based on total metal content were 3.1 h^{-1}, 0.2 h^{-1}, and 0.2 h^{-1}, respectively [17,46,47]. Dicationic imidazolium HPA ionic hybrid [Dmim]1.5PW behaved as a desirable heterogeneous catalyst, gave a 44 % conversion,100% selectivity with TOF value of 44 h-1 at 90 °C within 2 h using H_2O_2 as oxi-

Table 4. The benzyl alcohol conversion and benzaldehyde yield for complex (1) in the benzyl alcohol oxidation

Entry	Catalysts	Temperature (°C)	Pressure (bar)	Time (h)	Conversion (%)	Yield (%)
1	blank	100	3	2	9.3	3.2
2	complex (1)	90	3	2	37.3	36.9
3	complex (1)	100	3	1	23.4	23.3
4	complex (1)	100	3	2	65.6	54.3
5	complex (1)	100	3	3	85.6	66.3
6	complex (1)	100	1	2	47.7	45.8
7	complex (1)	100	5	2	69.5	19.5

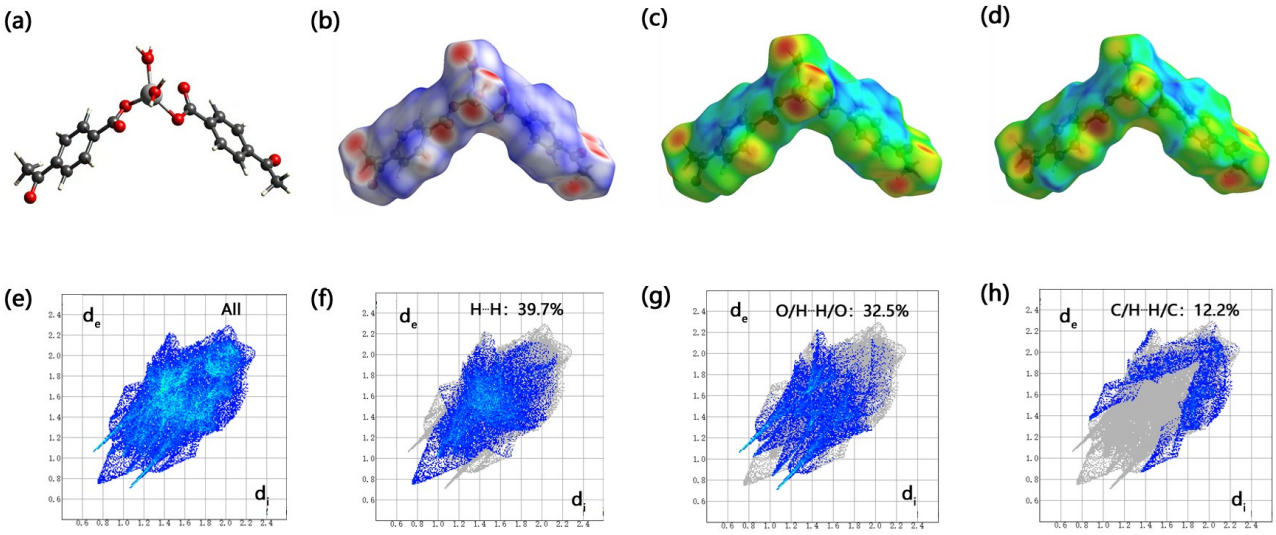

Figure 7. The Hirschfeld surface of the complex (1)

dant [48]. $H_3PMo_{12}O_{40}$ and $H_4PMo_{11}VO_{40}$ also showed good catalytic activity for the oxidation of benzyl alcohol at 80 °C using H_2O_2 as oxidant [49]. The benzyl alcohol conversions and benzaldehyde selectivities of $H_3PMo_{12}O_{40}$ and $H_4PMo_{11}VO_{40}$ were 22% and 99%, and 20% and 99%, respectively [49]. TOF values were 20.1 h^{-1} and 17.8 h^{-1} for $H_3PMo_{12}O_{40}$ and $H_4PMo_{11}VO_{40}$, respectively. Based on the above results, our complex (1) catalyst shows higher catalytic activity than $[Zn_3(L_1)_4(L_2)_2(CH_3COO)_2]$, $[Ca(L)_2(H_2O)_2]_n$, and $[BaL_2Cl_2]$. Although its TOF value is smaller than [Dmim]1.5PW, $H_3PMo_{12}O_{40}$, and $H_4PMo_{11}VO_{40}$, the catalyst shows good catalytic activity and yield to benzaldehyde using green oxidant O_2.

4. Conclusions

In summary, a new Zn(II) complex of 4-acetylbenzoic acid has been synthesized and characterized by IR and X-ray single-crystal diffraction analysis. Geometric parameters of complex (1) are all in good agreement with the experimental results. Selective oxidation of benzyl alcohol with complex (1) as catalyst shows that the highest benzaldehyde yield (66.3%) was obtained at 100 °C under 3 bar of O_2 after a runtime of 3 h.

Acknowledgments

This project was supported by National Natural Science Foundation of China (No. 21171132), Science Foundation of Weifang (2020ZJ1054) and Science Foundation of Weiyuan Scholars Innovation Team.

CRediT Author Statement

Author Contributions: Wang Li-Hua: Conceptualization, Methodology, Investigation, Resources, Data Curation, Writing, Review and Editing; Tai Hao-Wen: Investigation, Resources, Writing, Review and Editing, Validation. All authors have read and agreed to the published version of the manuscript.

References

[1] Wang, A., Hu, Z.J., Zhang, Y.T., Yuan, C.X., Feng, S.S. (2022). Synthesis, structures, corresponding fluorescence and magnetism of Zn(II) and Mn(II) coordination complexes based on 1-(3,5-dicarboxylatobenzyl)-1,2,4-1-H-triazole-3-carboxylic acid. *Inorganica Chimica Acta*, 542, 121112. DOI: 10.1016/j.ica.2022.121112

[2] Kokina, T.E., Glinskaya, L.A., Piryazev, D.A., Vasiliev, E.S., Sheludyakova, L.A., Rakhmanova, M.I., Tkachev, A.V. (2020). A complex of Zn(II) with chiral nopinane-annelated 9,9'-bi-4,5-diazafluorenylidene: synthesis, structure, and properties. *Journal of Structural Chemistry*, 61, 1606-1614. DOI: 10.1134/S0022476620100133

[3] Ajibade, P.A., Sikakane, B.M., Oluwalana, A.E., Paca, A.M., Singh, M. (2021). Synthesis, crystal structure and in vitro anticancer studies of bis(dibenzyldithiocarbamato)Zn(II). *Journal of Coordination Chemistry*, 74, 1244-1254. DOI: 10.1080/00958972.2021.1887482

[4] Alkış, M., Turan, N., Alan, Y., Irtegun, K.S., Buldurun, K. (2021). Effects of electroporation on anticancer activity of 5-FU and newly synthesized zinc(II) complex in chemotherapy-resistance human brain tumor cells. *Medical Oncology*, 38, 129. DOI: 10.1007/s12032-021-01579-7

[5] Mahmoud, M.A., Helal, M.A., Ammar, A.M. (2020). Zinc ternary complexes with gabapentin and neurotransmitters: Synthesis, spectral, thermal and molecular docking studies. *Journal of Solid State Chemistry*, 1199, 126951. DOI: 10.1016/j.molstruc.2019.126951

[6] Bhat, R.A., Singh, K., Kumar, D., Kumar, A., Mishra, P. (2022). Antimicrobial studies of the Zn(II) complex of S-benzyl-ß-(N-2-methyl-3-phenylallylidene)dithiocarbazate. *Journal of Coordination Chemistry*, 75, 1-13. DOI: 10.1080/00958972.2022.2083962

[7] Jaafar, A., Mansour, N., Fix-Tailler, A., Allain, M., Faour, W.H., Shebaby, W.N., Tokajian, S., El-Ghayoury, A., Naoufal, D., Larcher, G., Ibrahim, G. (2022). Synthesis, characterization, antibacterial and antifungal activities evaluation of metal complexes with benzaldehyde-4-methylthiosemicarbazone derivatives. *ChemistrySelect*, 7, 1-7. DOI: 10.1002/slct.202104497

[8] Holló, B.B., Radanović, M.M., Rodić, M.V., Krstić, S., Jaćimović, Ž.K., Ješić, V.L.S. (2022). Synthesis, physicochemical, thermal and antioxidative properties of Zn(II) coordination compounds with pyrazole-type ligand. *Inorganics*, 10, 20. DOI: 10.3390/inorganics10020020

[9] Sharma, H., Tamrakar, A., Maddeshiya, T., Shakya, P.R., Tiwari, K.K., D Pandey, M., Pandey, R. (2022). A zinc (II) complex comprising aminoethyl-nitropyridine derived N,N,O-donor schiff base ligand serves as an efficient ON-OFF probe for Cu(II). *Luminescence : the Journal of Biological and Chemical Luminescence*, 1-7. DOI: 10.1002/bio.4318

[10] Salga, M.S., Ali, H.M., Abdulla, M.A., Abdelwahab, S.I. (2017). Synthesis and gastroprotective activities of some zinc (II) complexes derived from (E)-2-(1-(2-(piperazin-1-yl)ethylimino)ethyl)phenol and (E)-4-(1-(2-(piperazin-1-yl)ethylimino)ethyl)benzene-1,3-diol Schiff bases against aspirin induced ulceration. *Arabian Journal of Chemistry*, 10, s1578-s1589. DOI: 10.1016/j.arabjc.2013.05.028

[11] Nasirian, A., Mirkhani, V., Moghadam, M., Tangestaninejad, S., Baltork, I.M. (2020). Efficient dye-sensitized solar cell based on a new porphyrin complex as an inorganic photosensitizer. *Journal of Chemical Sciences*, 132, 1-8. DOI: 10.1007/s12039-020-01781-6

[12] Nandanwar, S.K., Borkar, S.B., Wijaya, B.N., Bayarra, E., Piad, L.L.A., Jin, Q.L., Tiara, C.S., Hak J.K., Tarte, N.H. (2020). Synthesis and characterization of novel chelation-free Zn(II)-azole complexes: Evaluation of antibacterial, antioxidant and DNA binding activity. *Indian Journal of Chemistry*, 59A, 589-597.

[13] Zhao, M., Tan, J.Y., Su, J., Zhang, J., Zhang, S.Y., Wu, J.Y., Tian, Y.P. (2016). Syntheses, crystal structures and third-order nonlinear optical properties of two series of Zn(II) complexes using the thiophene-based terpyridine ligands. *Dyes and Pigments*, 130, 216-225. DOI: 10.1016/j.dyepig.2016.03.005

[14] Feng, S.S., Xie, L., Lu, L.P., Zhu, M.L., Su, F. (2018). The diversity of five metal-organic complexes based on an unsymmetrical biphenyl tetracarboxylate: Synthesis, structures, magnetism and luminescence. *Journal of Solid State Chemistry*, 258, 335-345. DOI: 10.1016/j.jssc.2017.10.035

[15] Bibi, S., Mohammad, S., Manan, N.S.A., Ahmad, J., Kamboh, M.A., Khor, S.M.,Yamin, B.M., Abdul Halim, S.N. (2017). Synthesis, characterization, photoluminescence, and electrochemical studies of novel mononuclear Cu(II) and Zn(II) complexes with the 1-benzylimidazolium ligand. *Journal of Molecular Structure*, 1141, 31-38. DOI: 10.1016/j.molstruc.2017.03.072

[16] Chaudhari, U.K., Bharti, A., Nath, P.A., Uday, P., Prakash, R., Butcher, R.J., Bharty, M.K. (2019). Synthesis, structure, photoluminescence and electrochemical properties of mononuclear Ag(I) and polymeric Zn(II) complexes of potassium 4-methyl piperazine-1-carbodithioate. *Journal of Molecular Structure*, 177, 260-268. DOI: 10.1016/j.molstruc.2018.09.055

[17] Wang, L.H., Kong, F.Y., Tai, X.S. (2022). Synthesis, crystal structure and Catalytic Activity of Tri-Nuclear Zn(II) Complex Based on 6-Phenylpyridine-2-carboxylic Acid and Bis(4-pyridyl)amine Ligands. *Bulletin of Chemical Reaction Engineering & Catalysis*, 17, 394-402. DOI: 10.9767/bcrec.17.2.13952.394-402

[18] Wang, L.H., Tai, X.S. (2022). Synthesis, crystal structure, hirschfeld surface analysis and catalytic activity of a new binuclear Zn(II) complex based on homophthalic acid and 2,2'-bipyridine ligands. *Bulletin of Chemical Reaction Engineering & Catalysis*, 17, 778-785. DOI: 10.9767/bcrec.17.4.16106.778-785

[19] Violeta Jevtović, V., Hamoud, H., Al-Zahrani, S., Alenezi, K., Latif, S., Alanazi, T., Abdulaziz, F., Dimić, D. (2022). Synthesis, crystal structure, quantum chemical analysis, electrochemical behavior, and antibacterial and photocatalytic activity of Co complex with pyridoxal-(S-methyl)-isothiosemicarbazone ligand. *Molecules*, 27, 4809. DOI: 10.3390/molecules27154809

[20] Wu, Y.F., Shi, S.B., Su, X.X., Zhang, Z.Q., Liu, P.L., Oderinde, O., Yi, G.Y., Xiao, G.M., Zhang, Y.L. (2021). Experimental and computational studies of Zn(II) complexes structured with Schiff base ligands as the efficient catalysts for chemical fixation of CO_2 into cyclic carbonates. *Molecular Catalysis*, 515, 111894. DOI: 10.1016/j.mcat.2021.111894

[21] Jadav, D., Shukla, P., Bandyopadhyay, R., Kubota, Y., Das, S., Bandyopadhyay, M. (2020). Tetranuclear Zn complex covalently immobilized on sulfopropylsilylated mesoporous silica: An efficient catalyst for ring opening reaction of epoxide with amine. *Molecular Catalysis*, 497, 111220. DOI: 10.1016/j.mcat.2020.111220

[22] Ma, Z., Aliyeva, V.A., Tagiev, D.B., Zubkov, F.I., Guseinov, F.I., Mahmudov, K.T., Pombeiro, A.J.L. (2020). Multinuclear Zn(II)-arylhydrazone complexes as catalysts for cyanosilylation of aldehydes. *Journal of Organometallic Chemistry*, 912, 121171. DOI: 10.1016/j.jorganchem.2020.121171

[23] Lee, J., Kim, D., Lee, H., Nayab, S., Hoon Han, J. (2022). Effect of initiator on the catalytic performance of zinc(II) complexes supported by aminomethylquinoline and aminomethylpyridine derived ligands in stereoselective ring opening polymerization of rac-lactide. *Polyhedron*, 216, 115696. DOI: 10.1016/j.poly.2022.115696

[24] Tai, X.S., Li, P.F., Wang, X., Liu, L.L. (2017). Synthesis, structural characterization, and catalytic property of a Zn(II) complex with 5-bromosalicylaldehyde ligand. *Bulletin of Chemical Reaction Engineering & Catalysis*, 12, 364-369. DOI: 10.9767/bcrec.12.3.876.364-369

[25] Subburu, M., Gade, R., Guguloth, V., Chetti, P., Ravulapelly, K.R., Someshwar, P. (2021). Effective photodegradation of organic pollutantsin the presence of mono and bi-metallic complexes under visible-light irradiation. *Journal of Photochemistry and Photobiology A: Chemistry*, 406, 112996. DOI: 10.1016/j.jphotochem.2020.112996

[26] Tai, X. S., Wang, X., You, H.Y. (2016). Synthesis, crystal structure and antitumor activity of a Zn(II) complex based on acetyl-L-phenylalanine and 1,10-phenanthroline. *Chinese Journal of Structural Chemistry*, 35, 586-590. DOI: 10.14102/j.cnki.0254-5861.2011-0910

[27] Tai, X.S., Guo, H.M., Guo, Q.Q. (2018). Synthesis, crystal structure and antitumor activity of a novel Zn(II) complex with 2-(nicotinoyloxy)acetic acid ligand. *Chinese Journal of Structural Chemistry*, 37, 1052-1056. DOI: 10.14102/j.cnki.0254-5861.2011-1880

[28] Wang, L.H., Wang, Z.J., Ouyang, J., Tai, X.S. (2021). The crystal structure of bis(6-phenylpyridine-2-carboxylate-k^{2}N,O)-(2,2'-bipyridine-k^{2}N,N')zinc(II) monohydrate, $C_{34}H_{26}N_4O_5Zn$. *Zeitschrift für Kristallographie -New Crystal Structures*, 236, 1297-1299. DOI: 10.1515/ncrs-2021-0312

[29] Tai, X.S., Zhou, X.J., Liu, L.L., Cao, S.H., Wang, L.H. (2020). The crystal structure of catena-poly[(μ$_2$-2-((3-bromo-2-oxidobenzylidene)amino)acetato-k^{4}O,N,O':O")-(dimethylformamide-k^{1}O)]zinc(II), $C_{12}H_{13}N_2O_4BrZn$. *Zeitschrift für Kristallographie -New Crystal Structures*, 235, 901-902. DOI: 10.1515/ncrs-2020-0090

[30] Tai, X.S., Li, P.F., Liu, L.L. (2018). Synthesis, crystal structure and catalytic activity of a calcium(II) complex with 4-formylbenzene-1,3-disulfonate-isonicotinic acid hydrazone. *Bulletin of Chemical Reaction Engineering & Catalysis*, 13, 429-435. DOI: 10.9767/bcrec.13.3.1961.429-435

[31] Tai, X.S., Li, P.F., Wang, X., Liu, L.L. (2017). Synthesis, structural characterization, and catalytic property of a Zn(II) complex with 5-bromosalicylaldehyde ligand. *Bulletin of Chemical Reaction Engineering & Catalysis*, 12, 364-369. DOI: 10.9767/bcrec.12.3.876.364-369

[32] Wang, L.H., Liang, L., Li, P.F. (2017). Synthesis, crystal structure, catalytic properties, and luminescent of a novel Eu(III) complex material with 4-imidazolecarboxaldehyde-pyridine-2-carbohydrazone. *Bulletin of Chemical Reaction Engineering & Catalysis*, 12, 185-190. DOI: 10.9767/bcrec.12.2.764.185-190

[33] Tai, X.S., Li, P.F., Liu, L.L. (2018). Preparation, characterization, and catalytic property of a Cu(II) complex with 2-carboxybenzaldehyde-p-toluenesulfonyl hydrazone ligand. *Bulletin of Chemical Reaction Engineering & Catalysis*, 13, 7-13. DOI: 10.9767/bcrec.13.1.1012.7-13

[34] Tai, X.S., Li, P.F. (2018). Synthesis, structure, and catalytic activity of a new Mn(II) complex with 1,4-phenylenediacetic acid and 1,10-phenanthroline. *Bulletin of Chemical Reaction Engineering & Catalysis*, 13, 1-6. DOI: 10.9767/bcrec.13.1.975.1-6

[35] Wang, L.H., Kong, F.Y., Tai, X.S. (2022). Synthesis, structural characterization of a new Ni(II) complex and its catalytic activity for oxidation of benzyl alcohol. *Bulletin of Chemical Reaction Engineering & Catalysis*, 17, 375-382. DOI: 10.9767/bcrec.17.2.13975.375-382

[36] Dolomanov, O.V., Bourhis, L.J., Gildea, R.J., Howard, J.A.K., Puschmann, H. (2009). *OLEX2*: A complete structure solution, refinement and analysis program. *Journal of Applied Crystallography*, 42, 339-341. DOI: 10.1107/S0021889808042726

[37] Sheldrick, G.M. (2015). SHELXT-Integrated space-group and crystal-structure determination. *Acta Crystallographica*, A71, 3-8. DOI: 10.1107/S2053273314026370

[38] Sheldrick, G.M. (2015). Crystal structure refinement with *SHELXL*. *Acta Crystallographica*, C71, 3-8. DOI: 10.1107/S2053229614024218

[39] Liu, M.R., Yue, E.L., Wang, J.J., Zhu, W.C., Quan, H., Tang, L., Wang, X., Hou, X.Y., Zhang, Y.Q. (2023). Selective detection of 2,4,6-trinitrophenol and fluazinam in water based on a 1D Zn(II) coordination polymer. *Chinese Journal of Inorganic Chemistry*, 39, 375-384. DOI:10.11862/CJIC.2023.002

[40] Adamo, C., Barone, V. (1999). Toward reliable density functional methods without adjustable parameters: The PBE0 model. *Journal of Chemical Physics*, 110, 6158-6170. DOI: 10.1063/1.478522

[41] Runge, E., Gross, E.K.U. (1984). Density-functional theory for time-dependent systems. *Physical Review Letters*, 52, 997-1000. DOI: 10.1103/PhysRevLett.52.997

[42] Casida, M.E. (1995). Recent Advances in Density Functional Theory (Part I), World Scientific, Singapore.

[43] Scalmania, G., Frisch, M.J. (2010). Continuous surface *charge* polarizable continuum models of solvation. I. General Formalism. *Journal of Chemical Physics,* 132, 114110. DOI: 10.1063/1.3359469

[44] Frisch, M.J., Trucks, G.W., Schlegel, H.B., Scuseria, G.E., Robb, M.A., Cheeseman, J.R., Scalmani, G., Barone, V., Petersson, G.A., Nakatsuji, H., Li, X.; Caricato, M., Marenich, A.V., Bloino, J., Janesko, B.G., Gomperts, R., Mennucci, B., Hratchian, H.P., Ortiz, J.V., Izmaylov, A.F., Sonnenberg, J.L., Williams-Young, D., Ding, F., Lipparini, F., Egidi, F., Goings, J., Peng, B., Petrone, A., Henderson, T., Ranasinghe, D., Zakrzewski, V. G., Gao, J., Rega, N., Zheng, G., Liang, W., Hada, M., Ehara, M., Toyota, K., Fukuda, R., Hasegawa, J., Ishida, M., Nakajima, T., Honda, Y., Kitao, O., Nakai, H., Vreven, T., Throssell, K., Montgomery Jr., J.A., Peralta, J.E., Ogliaro, F., Bearpark, M.J., Heyd, J.J., Brothers, E.N., Kudin, K.N., Staroverov, V.N., Keith, T.A., Kobayashi, R., Normand, J., Raghavachari, K., Rendell, A.P., Burant, J.C., Iyengar, S.S., Tomasi, J., Cossi, M., Millam, J. M., Klene, M., Adamo, C., Cammi, R., Ochterski, J.W., Martin, R.L., Morokuma, K., Farkas, O., Foresman, J.B., Fox, D.J. (2019). Gaussian 16, Revision C.01, Gaussian, Inc., Wallingford CT.

[45] Humphrey, W., Dalke, A., Schulten, K. (1996). VMD: visual molecular dynamics. *Journal of Molecular Graphics*, 14, 33-38. DOI: 10.1016/0263-7855(96)00018-5

[46] Tai, X.S., Guo, Q.Q., Li, P.F., Liu, L.L. (2018). A Ca(II) coordination polymer of 2-carboxybenzaldehyde:synthesis, crystal structure, and catalytic activity in oxidation of benzyl alcohol. *Crystals*, 8, 150-158. DOI: 10.3390/cryst8040150

[47] Wang, L.H., Tai, X.S., Liu, L.L., Li, P.F. (2017). Synthesis, crystal structure and catalytic activity of a novel Ba(II) complex with pyridine-2-carboxaldehyde-2-phenylacetic acid hydrazone ligand. *Crystals,* 7, 305-412. DOI: 10.3390/cryst7100305

[48] Leng, Y., Wang, J., Jiang, P. (2012). Amino-containing cross-linked ionic copolymer-anchored heteropoly acid for solvent-free oxidation of benzyl alcohol with H_2O_2. *Catalysis Communications*, 27, 101-104. DOI: 10.1016/j.catcom.2012.07.007

[49] Tong, J., Su, L., Li, W., Wang, W., Ma, H., Wang, Q. (2016). Hybrids of $[C_4mim]_{3+x}PMo_{12x}V_xO_{40}$: A new catalyst for oxidation of benzyl alcohol to benzaldehyde in water with greatly improved Performances. *Polyhedron*, 115, 282-287. DOI: 10.1016/j.poly.2016.05.024